Transonic Diffuser Case

Jacob Mills

November 5, 2020

1 Results from Wüthrich thesis

The case conducted by Wüthrich was based on the papers by multiple papers covering the simulation or numerical analysis of the same geometry and conditions. A paper by Bogar was used to determine the geometry and to provide experimental results for comparison. The thesis conducted a study on a weak shock case and a strong shock case. Do to issues with stability with the weak shock case and time constraints only the strong shock case will be discussed.

The thesis used the following formulas defined in a paper by Bogar to define the geometry of the diffuser.

$$\tilde{h}(\tilde{x}) = \frac{\alpha * \cosh(\zeta)}{(\alpha - 1) + \cosh(\zeta)} \tag{1}$$

$$\zeta = \frac{C_1(\tilde{x}/\tilde{l})(1 + C_2(\tilde{x}/\tilde{l}))^{C_3}}{(1 - \tilde{x}/\tilde{l})^{C_4}} \tag{2}$$

Table 1 shows the values used in equation 1 and 2. The paper gave bounds of between $x = -4.04$ and $x = 8.65$ with $x = 0$ being the point of connection between the converging and diverging sections of the diffuser. Wüthrich used unspecified bounds, as seen in Figure 1, instead of the bounds stated in the paper. The mesh used by the paper consisted of 10 blocks and had 81 x 51 volumes total (see Figure 1).

Table 1: Geometry calculations for the diffuser

Constant	α	l	C_1	C_2	C_3	C_4
Converging	1.4114	-2.598	0.81	1.0	0.5	0.6
Diverging	1.5	7.216	2.25	0	-	0.6

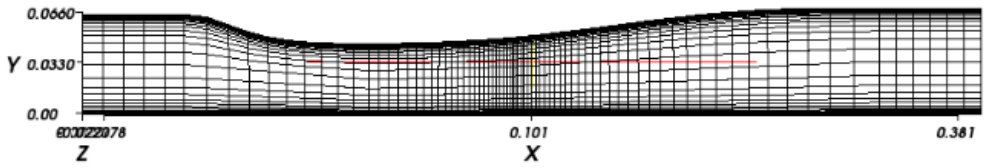

Figure 1: Mesh used in the the Wüthrich thesis

The strong shock case was run using **sonicTurbFoam** using a $k\epsilon$ solver. The resulting flow shows a standing shock appearing in the diverging section and abrupt change in velocity over the shock front. A separation of flow is also seen along the top wall of the diffuser (see Figure 2. Wüthrich points out that the shock was predicted a little to far downstream than where the experimental study found it to be in Bogar. **sonicTurbFoam** generally did a good gob at predicting the pressure along the bottom wall of the diffuser (see Figure 3). The graphs in Figure 4, showing the velocity at different x positions, show that **sonicTurbFoam** over predicted the velocities of the flow. No mesh refinement or validation study was conducted on case.

Table 2: Geometry calculations for the diffuser

Inflow		**OutFlow**	
Total pressure (kPa)	134.4	Static pressure, weak shock (kPa)	110.7
Total temperature (K)	277.8	Static pressure, strong shock (kPa)	97.2
Mach number	0.9		

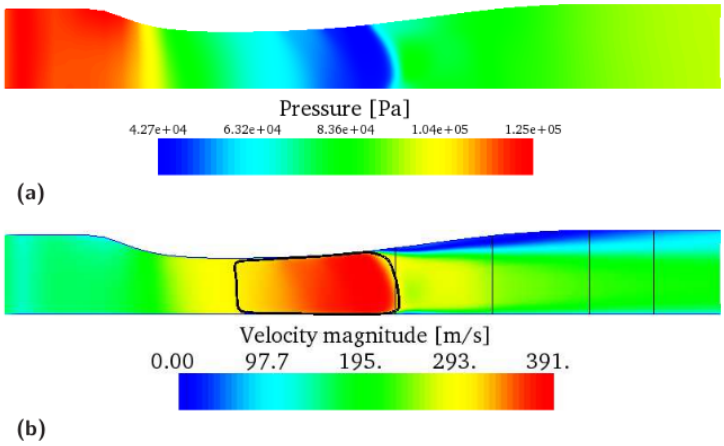

(a) x = 2.822

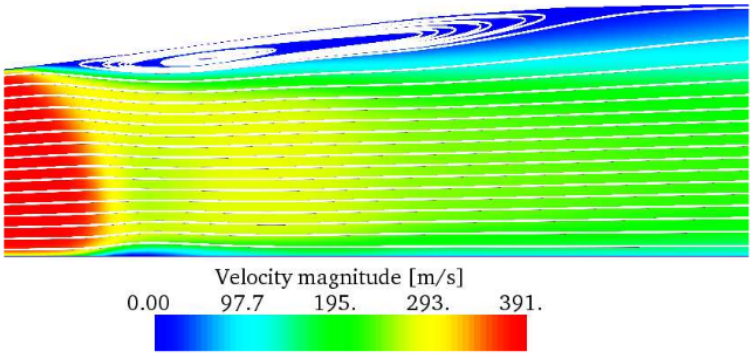

(b) x = 4.611

Figure 2: Velocity flood plots from the Wüthrich thesis.

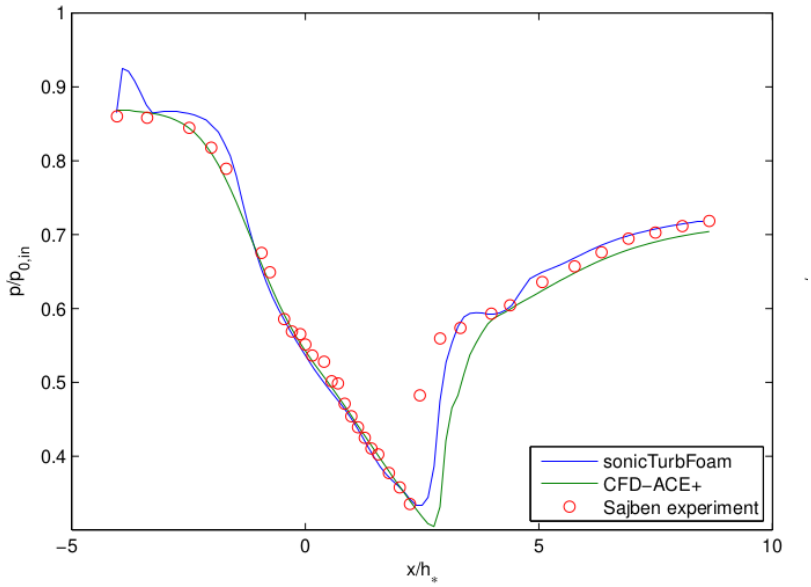

Figure 3: Plot of the pressure values at the bottom wall of the diffuser from the Wüthrich thesis.

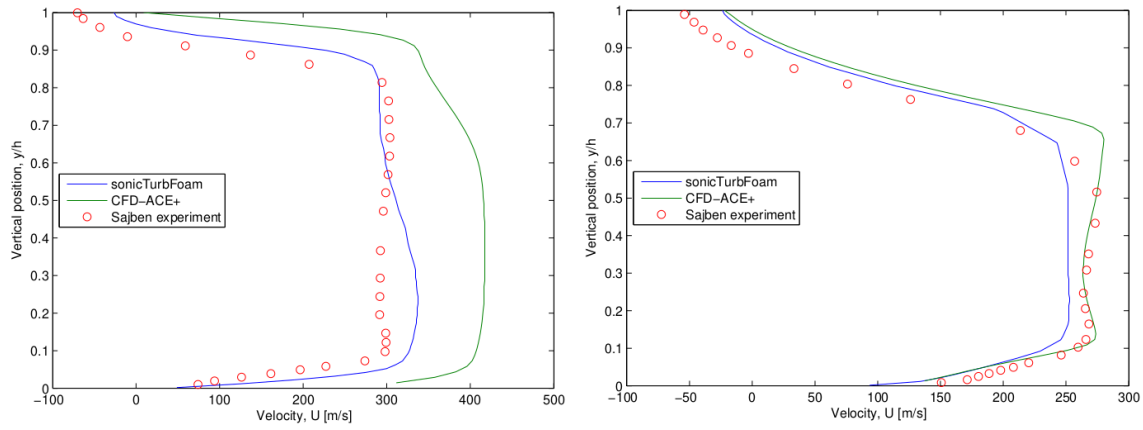

(a) x = 2.822

(b) x = 4.611

(c) x = 6.34

(d) x = 7.493

Figure 4: Plots at different x values of the velocity from the Wüthrich thesis.

2 Setup and Grid Generation

The grid used to recreate the study by Wüthrich was mad from one block and used multi-grading to grade the mesh. This was done to simplify the mesh and make it simpler to refine for the validation study. The coarse mesh was repeatedly run until a the mesh could be refined around the shock. The resultant mesh can be seen in Figure 5. The medium and fine grids were created by doubling the cell count (see Figure 3) and not changing the grading. This was done to keep the mesh as close to the one created by Wüthrich and to facilitate the validation study.

The **controlDict** file for the coarse, medium, and fine grids were set to run from $t = 0s$ to $t = 0.1s$ with both the medium and fine grids having their fields mapped from the coarse grid solution. As was expected, the medium and fine mesh required higher time steps than the coarse grid (see Table 3). An interesting observation was that the stable solutions for each grid has similar maximum Courant numbers when run at the maximum time step for the solution no to blow up. All cases were run on **sonicFoam**. The cases were not run on **sonicTurbFoam** due to it belonging to an earlier version of OpenFOAM while the current version of **sonicFoam** contains all the capabilities of **sonicTurbFoam**.

Table 3: Averaged residuals for the three cases.

Mesh	Cell Count	Time Step	Max Co
Coarse	81 x 51	$2e-06$	0.392
Medium	162 x 102	$1e-06$	0.399
Fine	324 x 204	$5e-07$	0.396

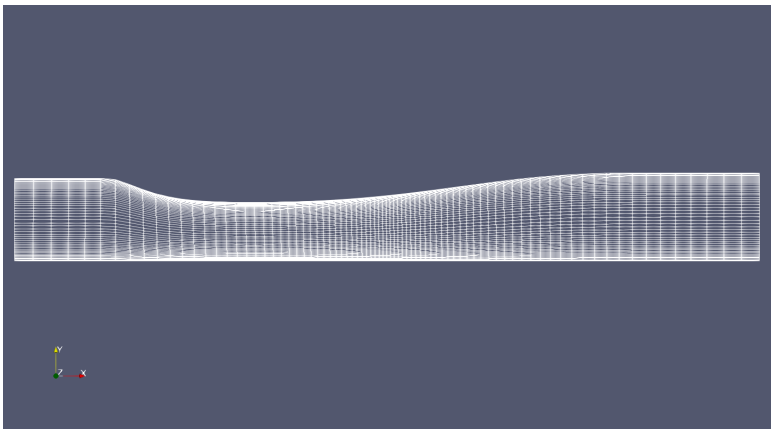

(a) Coarse Mesh

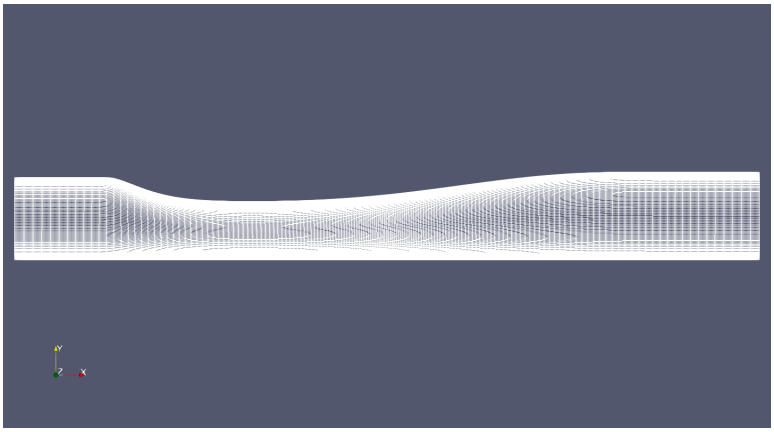

(b) Medium Mesh

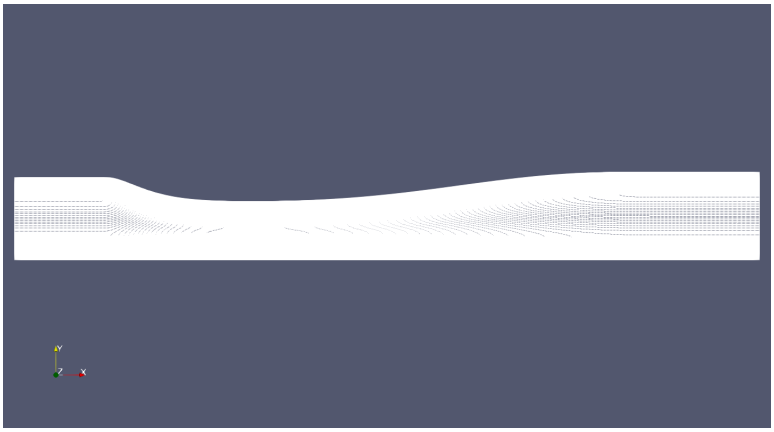

(c) Fine Mesh

Figure 5: Meshes generated. The cell count was doubled for each refinement.

3 Results

All three cases converged on a solution (see Table 4. In the coarse grid case, the solution behaved similarly to the Wüthrich solution where the solution's velocities were higher than the experimental around the shock (see Figure 9). Increasing the grid refinement only further exacerbated this and lead to each level of refinement caused the velocities to go higher. This can be further seen in Figure 6 showing that as the grid is refined the shock front moves further back. The shock front moving downstream has the effect of moving the high velocity zone in the immediate area upstream of the shock further downstream as well (see Figure7). This shift of the shock and the high velocity zone downstream correlates with Figure 9a showing the general increase in velocity with mesh refinement.

Generally **sonicFoam** tended to give closer solutions to the experimental the further downstream measurements were taken. This is especially true with the area close to the bottom wall of the diffuser which generally showed the best correlation. This higher level of precision can be seen in Figure 8 where **sonicFoam** predicts fairly well the pressure values close to the bottom wall. The Opposite can be said about the upper wall, as in each x position the **sonicFoam** solutions overestimated the velocity (see Figure 9). This region is where the flow separation occurs directly after the shock on the upper wall (see Figure 7).

Table 4: Averaged residuals for the three cases.

Mesh	$\mathrm{Ux}_{initial}$	Ux_{final}	$\mathrm{p}_{initial}$
Coarse	$5.017e-06$	$5.017e-06$	$1.887e-04$
Medium	$1.506e-06$	$1.506e-06$	$6.39e-05$
Fine	$7.101e-07$	$7.101e-07$	$3.148e-05$

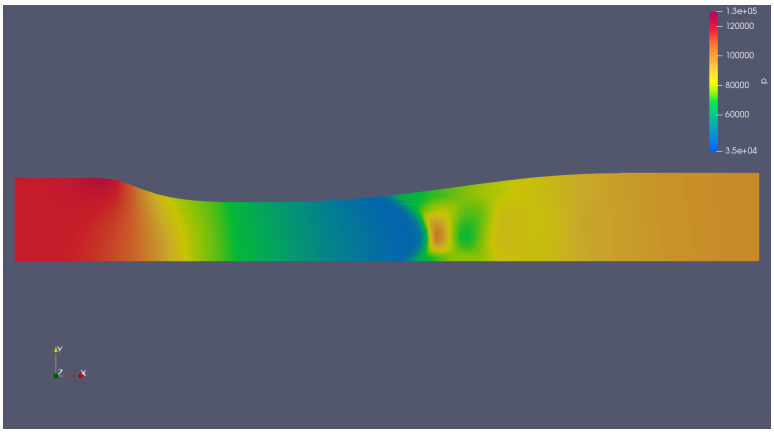

(a) Coarse Mesh

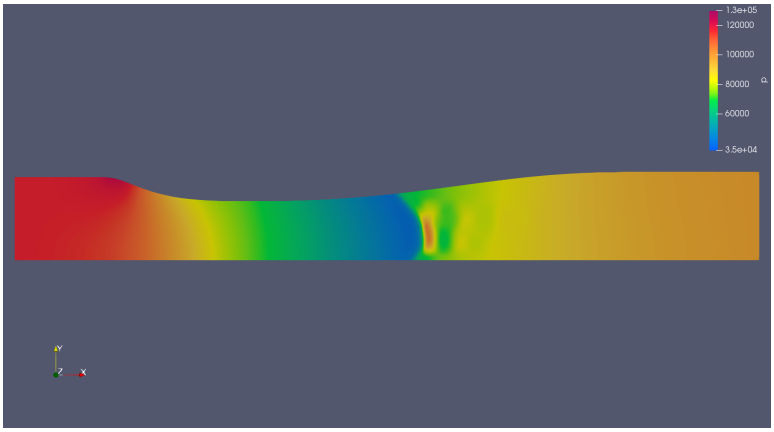

(b) Medium Mesh

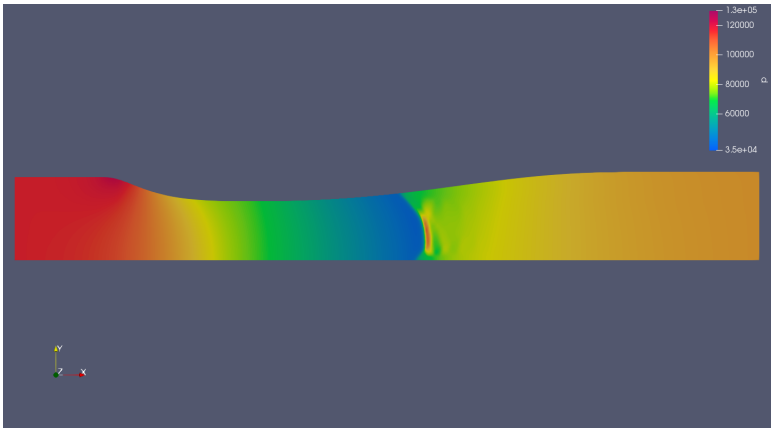

(c) Fine Mesh

Figure 6: Pressure flood plots.

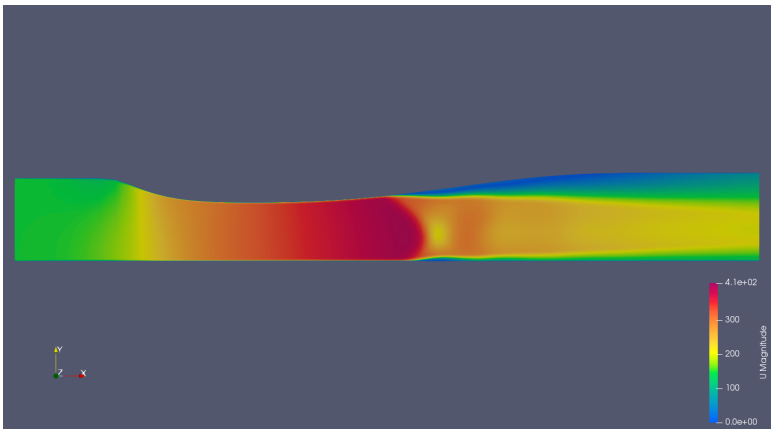

(a) Coarse Mesh

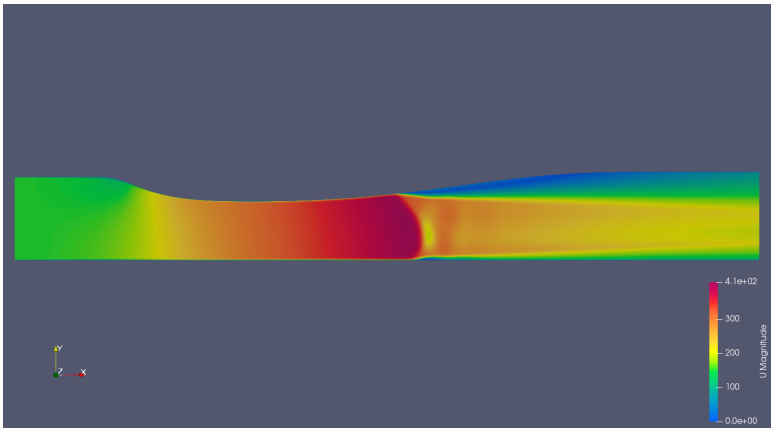

(b) Medium Mesh

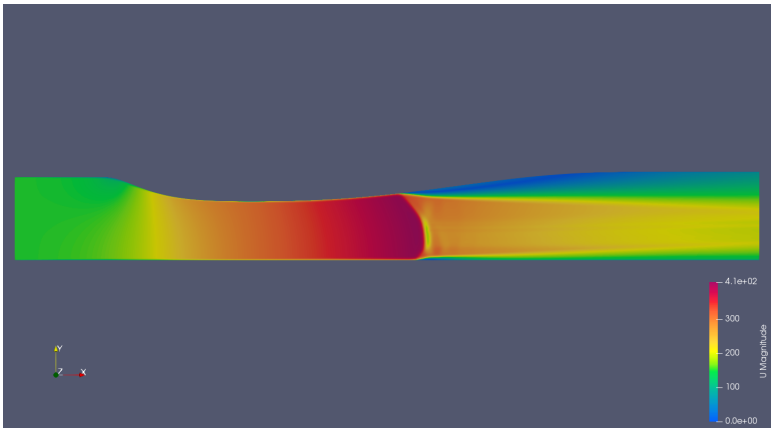

(c) Fine Mesh

Figure 7: Velocity flood plots.

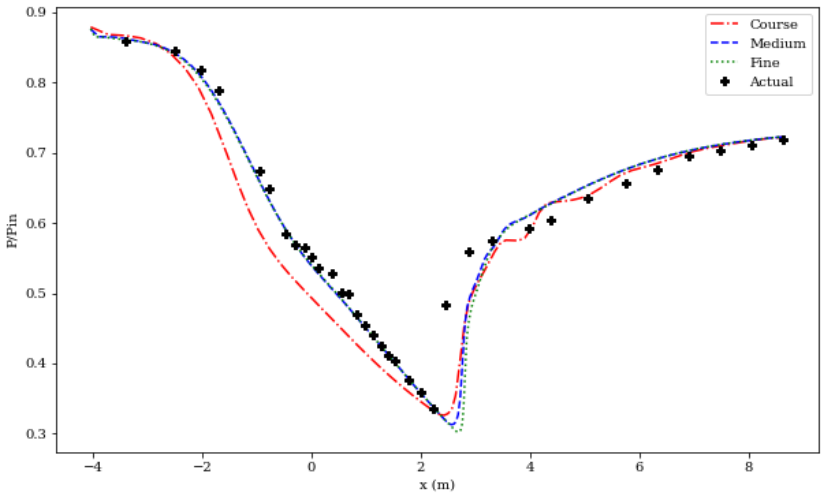

Figure 8: Plot of the pressure values at the bottom wall of the diffuser.

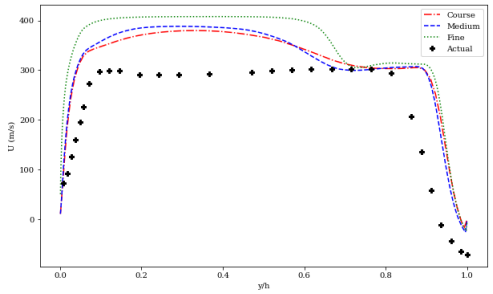

(a) $x = 2.822$

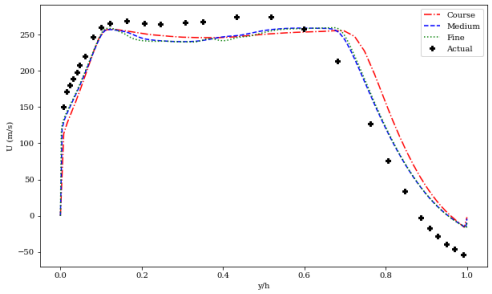

(b) $x = 4.611$

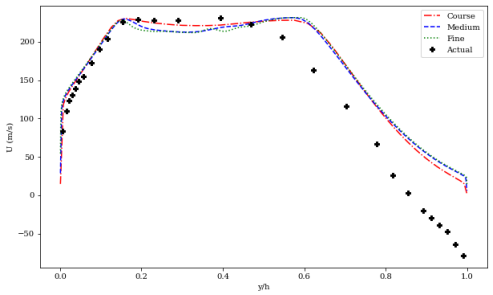

(c) $x = 6.34$

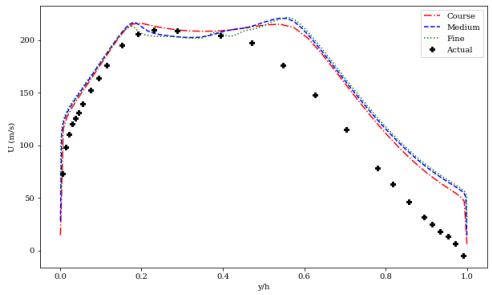

(d) $x = 7.493$

Figure 9: Plots at different x values of the velocity.

4 Validation

For the validation case p values were calculated for each x location the velocity was measured. This was then used to calculate GCI (see Table 5) values and a Richardson extrapolation of the data. The Richardson extrapolation was plotted alongside the **sonicFoam** coarse values as well as the actual (see Figure 10). The Richardson extrapolation shows similar results to the coarse mesh and follows similar trends. The extrapolation failed to show a significant improvement in accuracy. The error bars from the GCI are not very noticeable on the graph, leading to the possibility that they too small. The verification case shows that the errors coming up from the **sonicFoam** solver show a trend of overpredicting the velocity.

Table 5: Averaged p and GCI values

x Location	p_{avg}	GCI_{avg}^{coarse}	GCI_{avg}^{fine}
2.822	-1.885	5.13%	0.15.56%
4.611	2.29	1.74%	2.36%
6.34	1.22	-1.16%	0.053%
7.493	0.9384	0.93%	2.32%

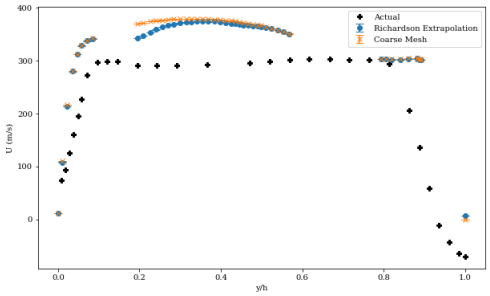

(a) $x = 2.822$

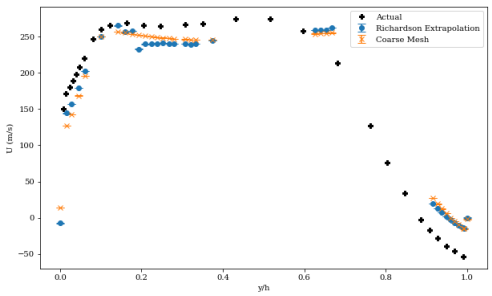

(b) $x = 4.611$

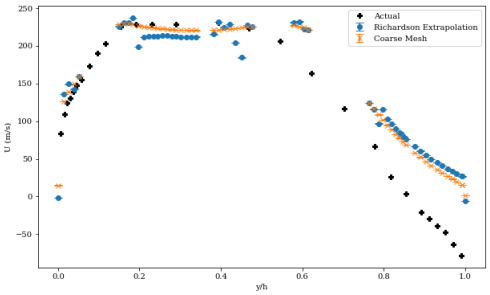

(c) $x = 6.34$

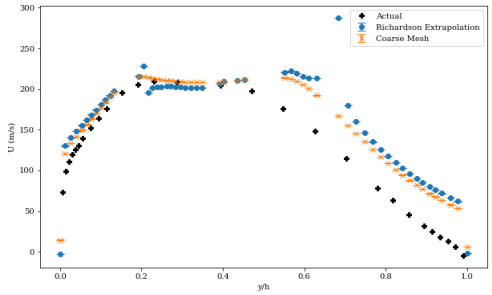

(d) $x = 7.493$

Figure 10: Plots at different x values of the velocity. Error bars are included to the Richardson extrapolation and coarse grid values.